Immobilization of a Molecular Pd Catalyst

Bachelor's Degree Project

Theodor Blom
Lund University

Project Duration: 6 Months, 15 hp

9 / 5 - 2016

LUND
UNIVERSITY

Prof. Joachim Schnadt
Department of Physics,
Division of Synchrotron Radiation Research,
Lund University

Payam Shayesteh
Department of Physics,
Division of Synchrotron Radiation Research,
Lund University

Contents

Abstract

In the past decade the term Green Chemistry has steered the direction of chemical industry and research. Green Chemistry is the idea of reducing environmental impacts of chemical reactions by lowering the energy consumption and reducing the amount of by-products. Nearly all industrial chemical processes use a catalyst in order to make their reaction more effecient. This study examines two different systems both developed to combine the aspects of Green Chemisty to the industry of catalysis through *supported homogeneous catalysis*. The overall goal is to simplify the separation of the catalyst from the reaction vessel through heterogenization and simultaneously increase the selectivity of the catalyst to reduce by-product creation. One system sees to determine the bonding geometry of a catalyst linker molecule on a silicon oxide model system through STM measurements in order to gain a deeper understanding of the immobilization of the catalyst. A crucial first step in inducing the heterogenization of the catalyst. The second system sees to examine the reusability of an already synthesised and immobilized polymer-embedded catalyst with increased selectivity by observing structural changes of the catalyst-complexes by SEM measurements. Due to a contamination problem in the STM chamber the linker molecule could not be dosed on the silicon oxide surface but important remarks were done regarding the preparation of the silicon oxide for future use. Some structural changes are observed on the polymer-embedded catalysts after consecutive reaction cycles, however, due to the small sample size of the study no major conclusions could be drawn.

1 Introduction

In recent years the term of green chemistry has become more established in the research and industry communities, and has hence been an overall aim for society as a whole. A whole journal dedicated to the field of green chemistry has even been instated by the Royal Society of Chemistry [9]. The term of green chemistry was popularised in 1998 through the publication of *Green Chemistry: Theory and Practice* by P. Anastas and J. Warner. In the book they discuss the twelve principles of green chemistry which would set the foundation for the chemistry in the years to come. The principles discussed in ref. [1] all convey a common goal of reducing waste products of chemical processes and reducing the impact of said chemical reactions by using environmentaly friendly resources.

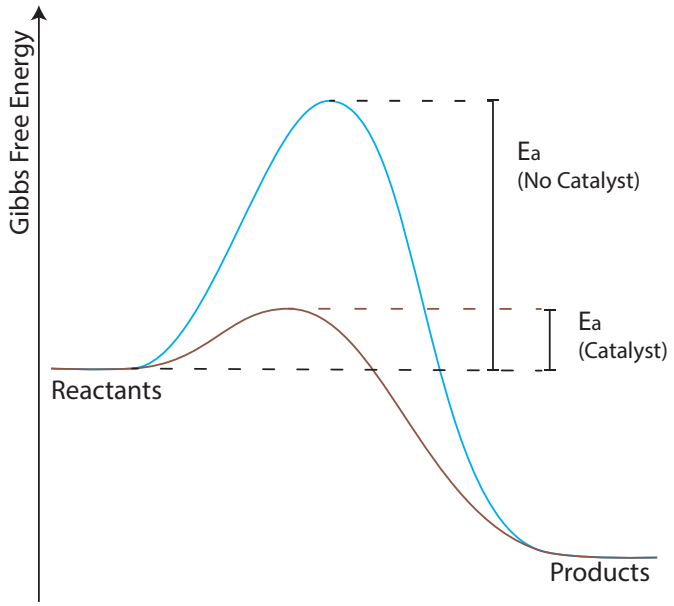

Figure 1: Energy diagram of an arbitrary chemical reaction shown with and without a catalyst. Without the catalyst the activation energy (E_a) for the reaction to happen is much higher than for the reaction with the catalyst.

A large proportion of the chemical industry today is governed by the use of catalysts to more efficiently implement the chemical reaction needed in the manufacturing procedure. A catalyst is a chemical compound (either a molecule or a surface) which assists in the reaction between other compounds by lowering the activation energy of the reaction. Figure 1 shows an illustration of this effect where, without a catalyst, the reactants must gain a significant amount of Gibbs free energy before being able to overcome the kinetic barrier. The Gibbs free energy is the energy of a system under constant temperature and pressure. The catalyst provides an alternative reaction mechanism where this kinetic barrier is lower. Hence more molecules have the energy required for reaction. In chemical reactions this kinetic difference has a considerable effect on the reaction rate of a chemical reaction and can lower the temperature required for a reaction to happen. In large scale processes this difference in temperature has a considerable effect on the energy consumption and is hence an advantageous choise.

Ever since the discovery of catalytic properties in certain materials they have been used to great extent and have been of important influence over the industrial development since the industrial revolution 200 years ago [6]. Due to the wide use of catalysis, it is a prime target for the application of the ideas captured by the concept of green chemistry.

There are many different catalysts each specific to a chemical reaction. They can roughly be divided into two major groups: heterogeneous- and homogeneous catalysts. As the names imply, homogeneous catalysts are in the same chemical state as the reactants and the products of the

reaction. In contrast, heterogeneous catalysts are not. In industrial applications the heterogeneous catalysts are most often preferred due to the simple separation process of the different phases of the final catalyst-product mixture. In the separation of homogeneous catalyst-product mixtures the catalyst is often lost among the byproducts of the reaction and must hence be re-synthesised.

In both a green chemistry and an industry perspective the heterogeneous catalysts are superior since they can be reused more times compared to the homogeneous catalysts and hence save both energy and resources. However, for a given reaction one can not decide preemptively if the catalyst for this reaction is homogeneous or heterogeneous. In more recent years research into the fields of *supported homogeneous catalysis* and *surface organometallic chemistry* has been made in an effort of combining these two catalyst types [2]. The long-term overall goal is to allow homogeneous catalysts to have the same benefit as heterogeneous catalysts by immobilization of the homogeneous molecular catalyst in a cavity of a zeolite structure.

Alongside the immobilization of the homogeneous catalyst, the goal here is to improve the selectivity of the catalyst by surrounding the immobilized catalyst in a rigid structure while maintaining access to the active site which allows the selection of a specific product. The selectivity of a catalyst is defined by the reaction rate of one product compared to the other availiable products of the same catalyst. From a set of reactants a catalyst could, for example, create different isomers of the desired product. Being able to select which product isomer should be more prominent in the reaction can hence severely decrease the amount of by-products from a reaction.

The selectivity of the immobilized catalysts is induced by attaching a template, structurally similar to the desired isomer of the product. A rigid structure, made of polymers for instance, is built around the catalyst and the template. If the surrounding structure is rigid enough, the removal of the template leaves a shape-specific hole called the active site. Due to the shape-specificity of the cavity, it favors the production of the product which is structurally similar to the template. The procedure would improve the catalyst beyond what traditional heterogeneous catalysts can do and has indeed been shown in previous research, cf. refs. [8] and [12].

The catalyst concerned in this project is a so called N-heterocyclic Carbene (NHC) -complex which consists of a metallic center surrounded by a number of NHC ligands. These ligands consist of carbon rings where one or multiple carbon atoms have been exchanged for a nitrogen atom. As reported by Hopkinson et. al. in a *Nature* article from 2014, the NHC ligands have found multiple applications within industrial catalysis since its isolation in 1991. The interest in NHC-complexes arose due to their characteristic property of acting as σ-bond donors binding to both metallic and non-metallic ligand centers which influence the stability, structure and reactivity of the formed complexes in a positive way [4]. These complexes are used more and more frequently within the field of homogeneous catalysis where they are coordinated to a transition metal center providing the catalytic activity. As discussed earlier, the homogeneous catalysis has alot of potential area of improvments from both a green chemistry and a industrial perspective in a catalytic reaction. The goal of this study is to examine the possibilities of applying the ideas of supported homogeneous catalysis to these types of homogeneous catalysts.

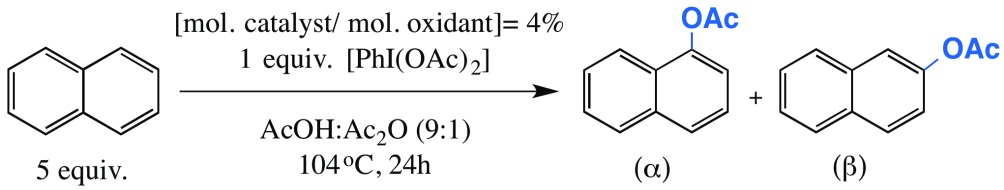

Figure 2: Schematic of the chemical reaction being catalysed by the concerned catalyst where an hydrogen atom on the naphtalene molecule is exchanged to an acetoxy group which can result in two different availiable products.

The reaction in focus is illustrated in figure 2 above where a naphtalene molecule reacting with a mixture of acetic acid and acetic anhydride can form two different resulting isomers. The goal is to increase the catalyst selectivity while maintaining the catalyst activity (the rate of which a certain amount of product is produced). To achieve this two different methods were developed both striving towards the same goal.

In the first method, the catalyst is modified to contain a linker molecule which assists in the attachement of the molecule to a siliconoxide surface. The linker molecule can be seen in figure 5. Using the linker the catalyst is immobilized on the surface and thus the catalyst is heterogenized. If the catalyst is oriented on the surface in such a way that the reactive part is along the normal to the surface the template can be attached and rigorous walls can be built around the catalyst to induce selectivity. In the present project the goal is to achieve the building of this rigid structure by a process called Atomic layer deposition (ALD) [5].

The second method of immobilization uses carbon polymers to both assist in the heterogenisation and induce the selectivity of the catalyst. A schematic image of the polymer embedded catalyst can be seen in figure 6. By surrounding the molecular catalyst in a polymer matrix the matrix is more distinguishable in a product-catalyst mixture and can hence be separated by its size and be reused. Applying the same idea of attaching a shape-specific template before building the polymer matrix induces the selectivity.

The first aspect of this work is to study the initial stages of the first method of immobilization and to examine the bonding of the linker to the silicon oxide surface. This is done by scanning tunneling microscopy where the linker molecule is dosed onto a silicon oxide surface with a few monolayers of oxide and is compared with the pure silicon oxide for the deduction of the bonding geometry. These initial steps are taken in preparation for the synthesis of the complete catalyst. The silicon oxide surface is a model system on which the bonding geometry of the linker can easily be examined.

Furthermore, in this work the polymer-embedded catalysts, which have been synthesised and are used in the reaction specified by figure 2, have been characterized. The catalytic activity of the catalyst was examined for each reaction cycle and after each consecutive reaction cycle the polymer complexes are extracted from the product mixture. The extracted catalysts are examined by scanning electron microscopy to identify any possible structural changes of the complex in order to determine the reusability of the polymer complexes.

2 Methods

2.1 Experimental Techniques

In order to examine the the properties of the systems described above, scanning tunneling microscopy and scanning electron microscopy were used. Here follows a brief introduction to these experimental techniques.

2.1.1 Scanning Tunneling Microscopy

As illustrated in figure 3, scanning tunneling microscopy (STM) uses the tunneling capabilities of electrons to image a surface on the atomic scale. By application of a voltage between tip and sample, the tip can be approached towards the surface using a piezoelement until a set tunneling current of a few nA is achieved. Due to the potential barrier, the tunneling current is exponentially decaying over the tip-surface distance d.

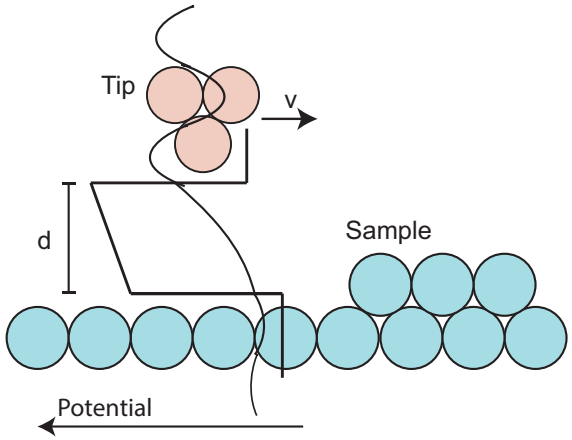

Figure 3: Schematic figure of the STM technique showing the tip (red) interacting with the surface (blue) through electron tunneling. The tunneling current is exponentially decaying over the potential gap of width d and is proportional to the density of states of the sample. In constant-current mode, to avoid collisions, the distance d is adjusted for the changing current.

A crucial parameter in obtaining the atomic resolution is the condition of the tip being scanned over the surface. The tip of the STM tip must only be one atom thick such that the tunneling current originates from a restricted area. Thus the tunneling current can be seen as one dimensional. For a current to be induced the chemical potentials (μ) of tip and surface must be different. Thus, application of a voltage between the tip and surface induces a tunneling current across the potential barrier. The current (I) is proportional to the density of states (ρ) of the sample according to Bardeen's tunneling theory [3]:

$$\begin{aligned} I &= (\mu_t - \mu_s)\frac{eh^3}{m^2}A^2\rho_{tip}(\mu)\rho_s(\vec{0},\mu)\ , \\ \text{where}\quad \rho_s(\vec{r},\mu) &= \frac{1}{|\mu_s-\mu_t|}\sum_{\psi_n:\mu_a<\varepsilon_n<\mu_b}|\psi_n(\vec{r})|^2. \end{aligned} \tag{1}$$

Equation one above indicates that the tunneling current (I) depends on many factors related to the tip and the sample. However, during an ideal measurement the chemical potential (μ) of both tip and sample and the tip area (A) is constant, which restricts the change in current to the density of states ($\rho_s(\vec{r}, \mu)$). The one dimensionality of the current then allows for imaging of the density of states on the atomic scale which reveals the atomic structure of the sample.

When the desired tunneling current is achieved after approach, scanning can be initiated. A common scanning mode is called a constant-current mode where the tip- surface distance d is manipulated by the piezoelement in order to keep the tunneling current constant. This is made possible by the exponential dependancy of the current over the distance d.

2.1.2 Scanning Electron Microscopy

Scanning electron microscopy (SEM) uses the scattering which occurs during the electron-matter interaction to produce an image of a sample. As is shown in figure 4, electrons are accelerated towards a sample and focused through a set of electron condenser lenses and deflection coils onto the sample to a focus point on the scale of a few nanometers in diameter. The scanning mechanism of the focusing coils allows for quick imaging of the sample.

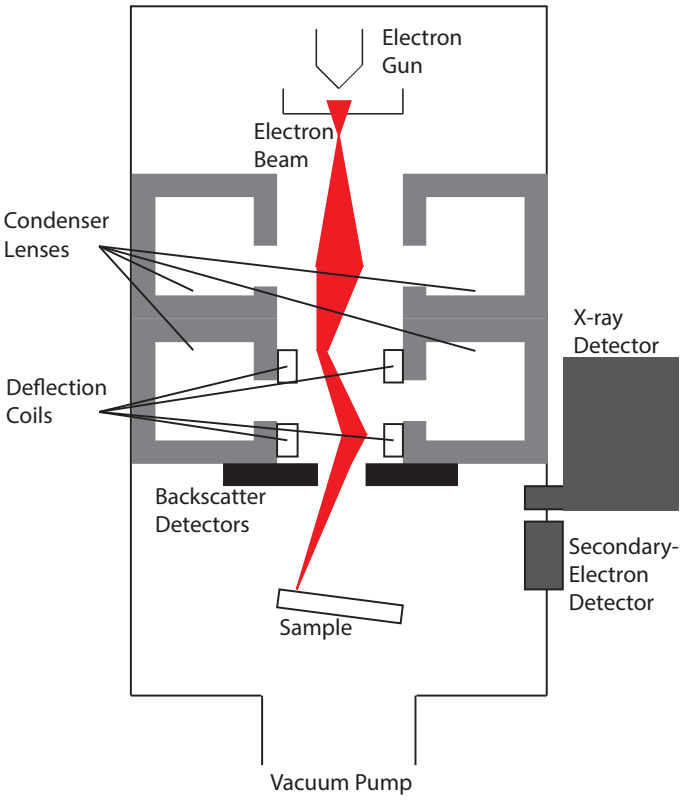

Figure 4: Schematic image of an scanning electron microscope. Image adapted from [15].

The electron-matter interaction produces three main types of radiation able to be detected by detectors placed in the sample chamber: primary backscattered electrons, secondary electrons and photons. Taking advantage of the combination of the three different detectors allows the scanning electron microscope to provide spatial contrast images which can show the elemental composition of the sample. The most common imaging technique measures inelasticly scattered secondary electrons from different angles to produce the spatial contrast image of the sample. These electrons originate from the surface of the sample and through measurement of the energy and phase of these electron an image with a spatial resolution on the 10 nm-scale can be achieved [13].

2.2 Experimental Setup

Two main measurement techniques were used. For the examination of the bonding of the linker molecule on the silicaoxide surface a scanning tunneling microscope at Lund University was used. To detect any structural changes of the polymer-embedded catalysts after each consecutive reaction cycle a scanning electron microscope was used. In order to avoid electron scattering effects in the SEM and have more control of species on the silica surface for the STM, both of these techniques were used in the ultrahigh vacuum (UHV) regime ($10^{-10} - 10^{-11}$mbar).

The scanning tunneling microscopy measurements were carried out in a vacuum chamber able to sustain UHV conditions with both access to STM as well as low-energy electron diffraction (LEED). The UHV conditions of the main vacuum chamber was sustained by an Agilent Technologies TwisTorr 304 TS Turbopump along with an ion pump with an available Titanium Sublimation Pump (TSP). The pressure in the chamber was measured by a Pfeiffer Vacuum Compact Cold Cathode Gauge. Connected to the vacuum chamber was a gas inlet system with four available gas inlets each connected to a Duniway Stockroom leak valve for accurate dosage of gas into the chamber. Furthermore, the chamber was equipped with a MolecularSpray electrospray deposition system for depositing the catalyst onto the surface.

The scanning electron microscopy measurments were performed on the high resolution scanning electron microscope Nova Nanoab 600 located at the Lund Nano Lab. See section 2.1.2 for a description of a scanning electron microscope.

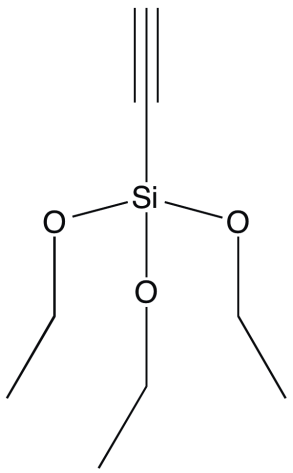

Figure 5: Catalyst linker molecule. Schematic of the chemical composition of the linker molecule triethoxyethynylsilane (TEES) used to attach the catalyst to the oxidised silicon surface.

2.3 Preparations and Measurements

2.3.1 Scanning Tunneling Microscopy

The vacuum chamber described earlier was evacuated and baked to reach a pressure in the low 10^{-10} mbar regime and the electrospray was mounted on the chamber. The p-doped Si(001) wafer was cut into a rougly 5 mm × 15 mm-sized wafer and cleaned by sonication for 10 min. The sample was mounted on the sample holder designed for electrically heating the sample by application of a voltage across the sample inducing a current (Joule Heating). Precautions for avoiding contaminants on the sample were taken during the whole preperation procedure by minimizing contact between the sample and other materials.

The sample was loaded into the vacuum chamber and was heated to 700 °C and left at this temperature over 15 h. Since the samples were taken form atmospheric pressure, also species other than oxygen are adsorbed on the surface. Leaving the sample at 700 °C allows for the desorption and removal of these species from the vacuum chamber [7]. Since a majority of these species are hydroxyl-groups this procedure is called dehydroxylation. The sample was then flash-annealed at 1100 °C to remove the remaining oxide layer [14] and was transfered to the STM measurement area for

imaging.

One of the gas inlets of the chamber was filled with pure oxygen and application of a few monolayers of oxygen was undertaken according to a previously proposed recipe [10]. The sample was heated to 600 °C and re-oxidised under a pressure of $5 \cdot 10^{-8}$ mbar dosing different amounts of oxygen onto the surface measured in Langmuirs ($1\ \mathrm{L} = 10^{-6}\ \mathrm{torr} \cdot \mathrm{s}$). This in order to achieve a controlled oxide layer such that the bonding geometry of the linker can be examined in more detail.

The newly oxidised silica surface was exposed to the linker molecule as seen in figure 5. Due to the high vapor pressure of the linker molecule the exposer was done by letting the molecule evaporate into the chamber for different amounts of Langmuirs.

The cleaning, oxidation and linker dosing procedures were repeated with different parameters on the amount of Langmuirs dosed, both for oxidation and linker dosing. Between each step the sample was transfered to the STM area of the chamber for varification of the success of the performed step.

2.3.2 Scanning Electron Microscopy

The catalyst polymer matrix shown in figure 6 was prepared where the Pd-catalyst along with the template is embedded in a polymer matrix of carbon chains. The template was removed and the catalyst was used in the catalytic reaction shown in figure 2. Some of the polymer embedded catalysts were then extracted and placed on a surface. This procedure was repeated four times such that four different samples of the catalyst extracted from consecutive reaction cycles could be made.

In preparation for the SEM measurements the four samples were coated in a layer of Pt using a sputter-coating technique creating a layer of a few monolayers. The samples were coated in the conductive Pt to avoid charging effects on the SEM images. The four different samples were placed in the scanning electron microscope for characterization.

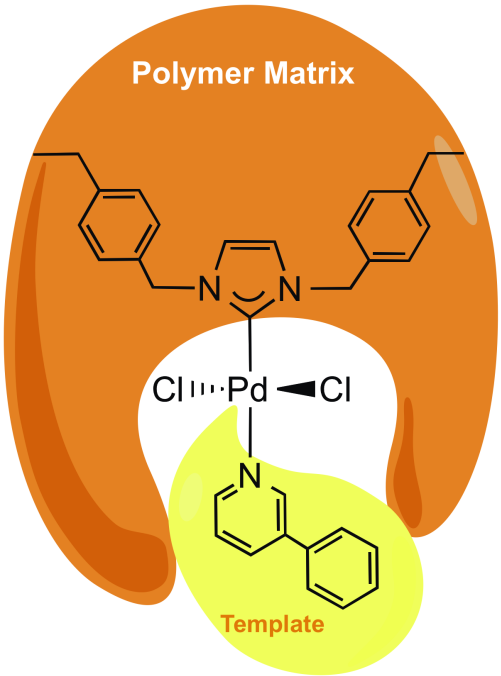

Figure 6: Schematic of the chemical composition of the polymer embedded catalyst. The template is used to form the cavity increasing the selectivity of the catalyst.

3 Results and Discussion

3.1 Scanning Tunneling Microscopy

The Si(001) (2×1) surface, onto which the linker molecule later will be adsorbed, was dehydroxylized and flash-annealed to remove the oxide-layer situated ontop of it by being exposed to atmospheric pressure.

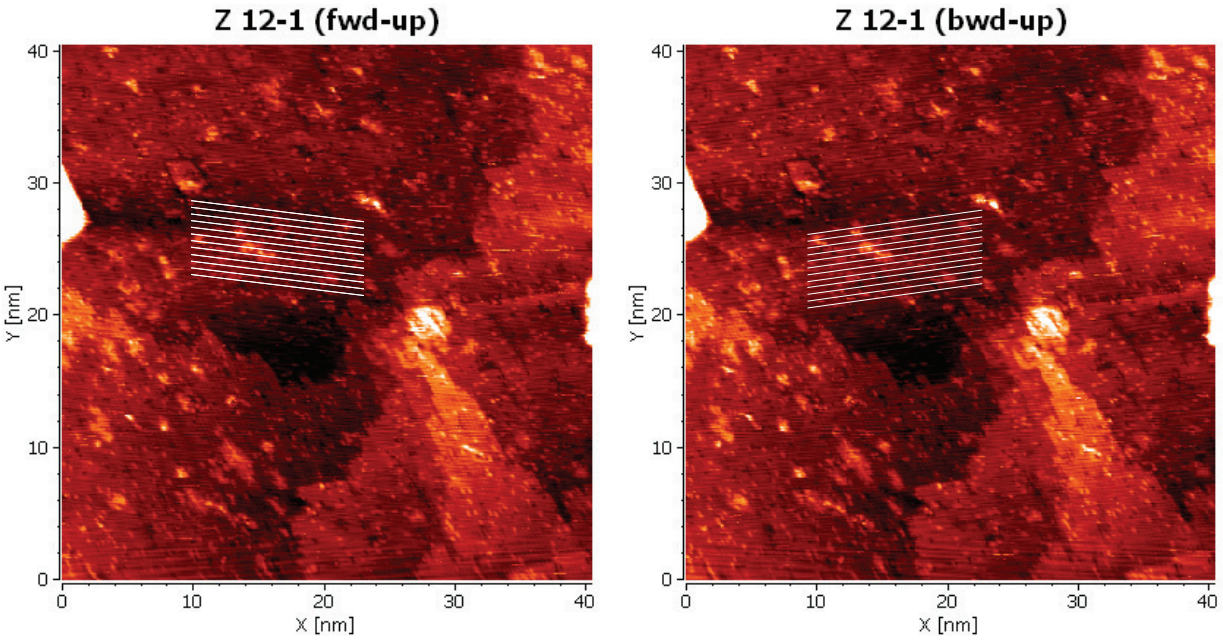

Figure 7: STM image of the dehydroxylated and flash-annealed Si(001) (2 × 1) surface in the forward and backward scanning directions. White lines indicate the orientation of the vibrational lines originating from vibrations in the experimental setup.

In order to confirm the validity of the proposed cleaning procedure described in section 3.2.1, an STM image of the clean Si(001) (2 × 1) surface was taken and is shown figure 7 above. The image to the right is compiled of all the line scans done when the tip was scanning in the forward scanning direction and the image to the left is taken in the backwards scanning direction. In both images one can observe what seems to be atomic rows as indicated by the white lines; however, in the two images the rows seem to be directed in different directions one being tilted to the right and one being tilted to the left indicating otherwise. This effect is explained by the thermal vibrations of the tip-sample mechanism setup distorting the atomic resolution of the image. By scanning in both scanning directions this effect can be detected.

In some regions of the images the mechanical vibrations does not seem to have an effect and the rows are tilted in the same directions for both images. In figure 8 below one of these regions without vibrations have been enhanced for better view.

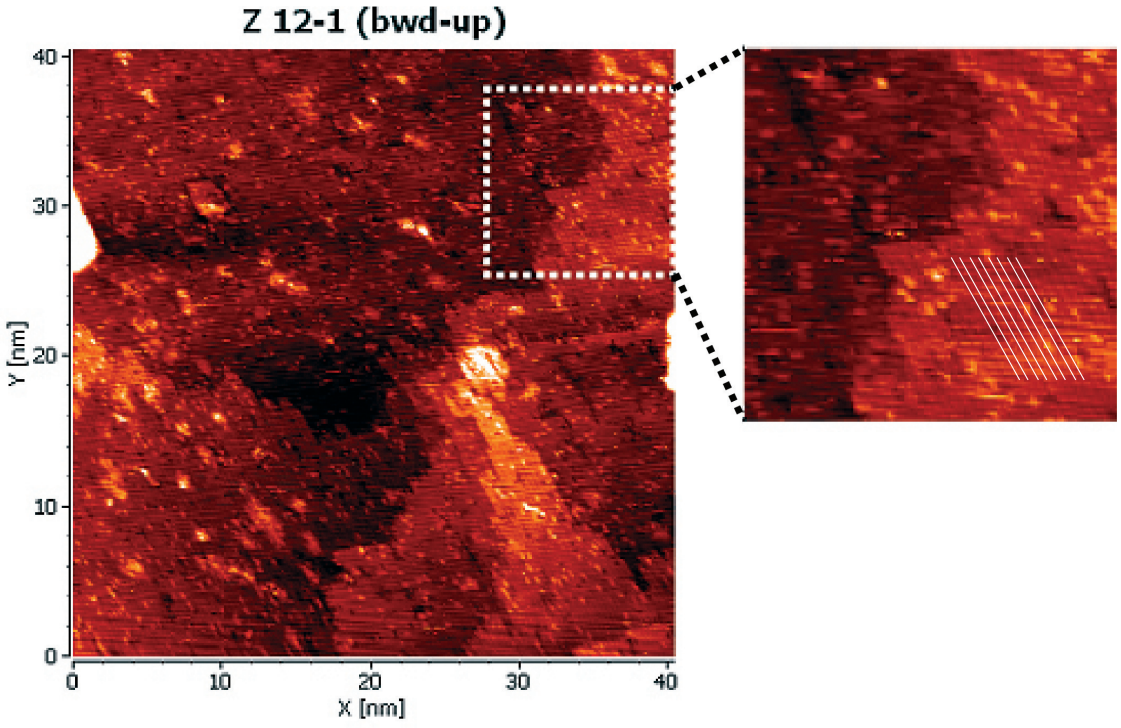

Figure 8: Cut-out of figure 7 showing an area where lattice vibrations do not interfer with the atomic resolution. In the area the Si(001) construction can be seen.

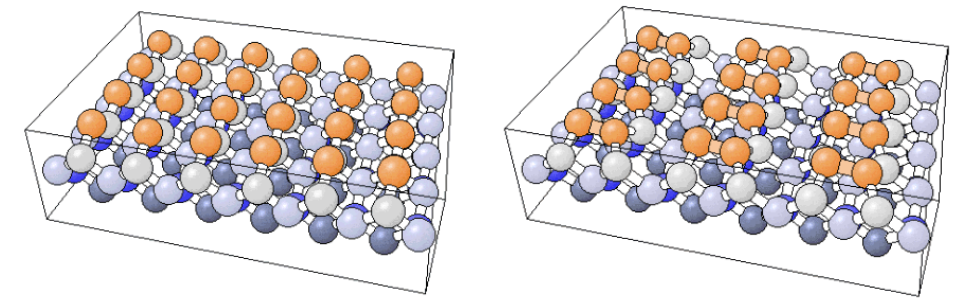

Figure 9: Theoretical illustration of the Si(001) (1×1) (left) and Si(001) (2×1) reconstruction (right). Images taken from WWW Picture gallery based on in the Surface Structure Database (SSD, NIST Standard Reference Database 42) by P. R. Watson, M. A. Van Hove, K. Hermann. The pictures have been prepared from SSD output and postprocessed with BALSAC by K. Hermann.

Comparison of the zoomed-in image from figure 8 with the (001) structure of the fcc- lattice in figure 9 indicates that a clean Si(001)-surface has been achieved in figure 8. Due to the relaxation of the surface atoms, the (2×1) recontruction is observed rather than the (1×1) reconstruction. The comparison confirms the validity of the cleaning procedure proposed in refs. [7] and [14] of dehydroxilation and removal of the oxide layer. Comparison with earlier studies on the Si(001)

(2×1) surface in ref. [11] also confirms the clean Si(001) (2×1) surface seen in figure 8.

The STM images also contain bright spots which does not seem to be silicon atoms. Analysis of figure 7 reveals a bright spot coverage of roughly 5% which is deemed sufficiently low to be explained by the pressure in the chamber being in the 10^{-9} mbar regime after flash-annealing. This pressure is too high for the Si-surface not too react with the residual molecules in the chamber during cooling the sample to room temperature and transfering it to the STM area which was rougly 30 min. The residual molecules in the chamber are most likely oxygen, but further investigation must be done to verify. The contamination of the clean Si(001) surface could be avoided by maintaining the lower pressure in the experimental station through for example having a separate preparation chamber not to interfere with the pressure of the main chamber.

Furthermore, the surface in figure 7 and 8 exhibits terraces on the order of roughly 10 nm. To establish the small terraces of the surface a statistical analysis must be made. However, due to difficulties regarding the STM only a few images of the clean Si- surface could be aquired and can hence not be said with certainty. The terrace length of many crystalline surfaces can be used as an indicator for how successful the cutting of the crystal was. The short terrace length could prove as a disadvantage for the pending catalyst due to the difficulties of obtaining a smooth oxide layer. In turn the rough oxide layer could hinder an optimal bonding orientation of the catalyst. Terraces of at least 100 nm would be prefered.

The re-oxidation of the Si-surface was carried out, but did not result in usable images due to lack of time. After oxidation of a few Langmuirs at 600 °C no structure on the surface could be seen. Flash annealing the sample after re-oxidation did not yield the previous results as shown in figure 7 and 8 indicating either scanning/tip failure or contaminants other than oxygen in the chamber.

3.2 Scanning Electron Microscopy

Concerning the polymer-embedded catalysts, the four samples containing the catalyst complexes each extracted from a consecutive reaction cycle described earlier was loaded into the scanning electron microscope for imaging. Figures 10 through 13 show the resulting SEM images from the consecutive reaction cycles of the polymer embedded catalysts.

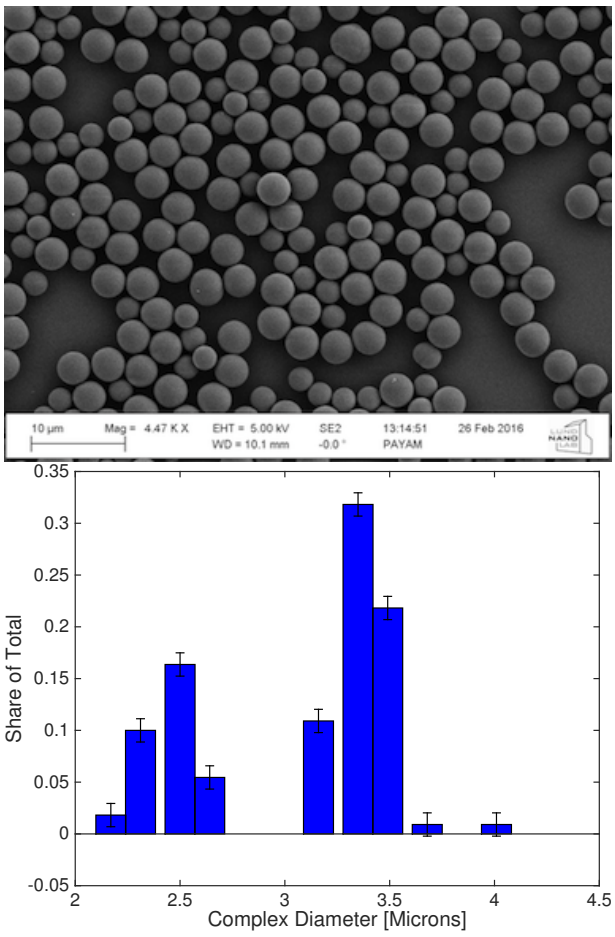

Figure 10: SEM image of the polymer-embedded catalyst complexes extracted after the first reaction cycle along with its size distribution histogram with a sample size of 110. See scale in the bottom left of the SEM image for size comparisson.

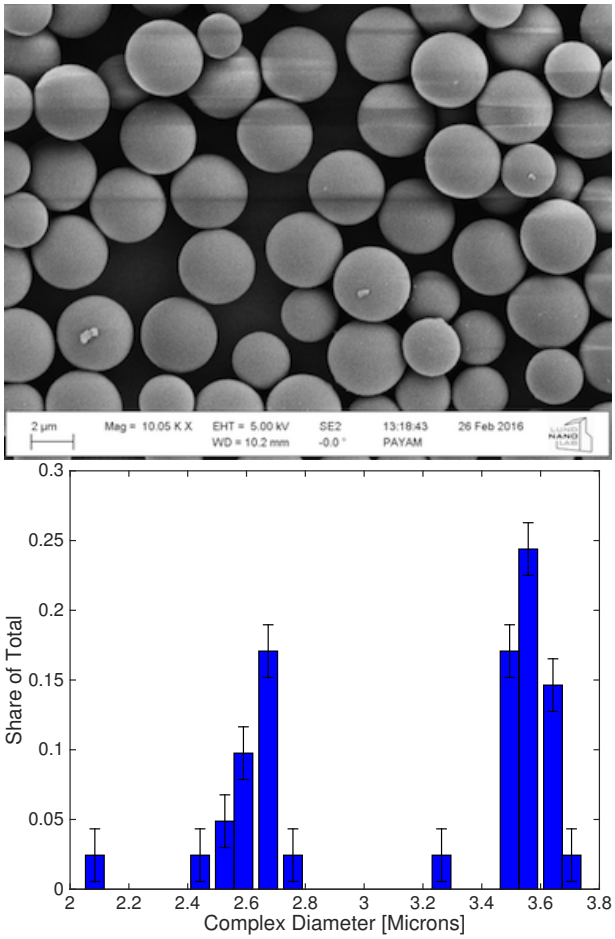

Figure 11: SEM image of the polymer-embedded catalyst complexes extracted after the second reaction cycle along with its size distribution histogram with a sample size of 41. See scale in the bottom left of the SEM image for size comparisson.

In figures 10 and 11 the catalyst complexes extracted after cycle 1 and cycle 2 can be seen respectively. Comparing the catalyst complexes between the the two consecutive cycles directly reveals no macroscopic structural change. A statistical analysis of the complex sizes reveals a complex

diameter in the range of 2 - 4 µm seemingly in two distributions around 2.6 ± 0.15 µm and the other 3.5 ± 0.15 µm. However, a larger sample amount is needed to confirm if the distribution is of statistical relevancy.

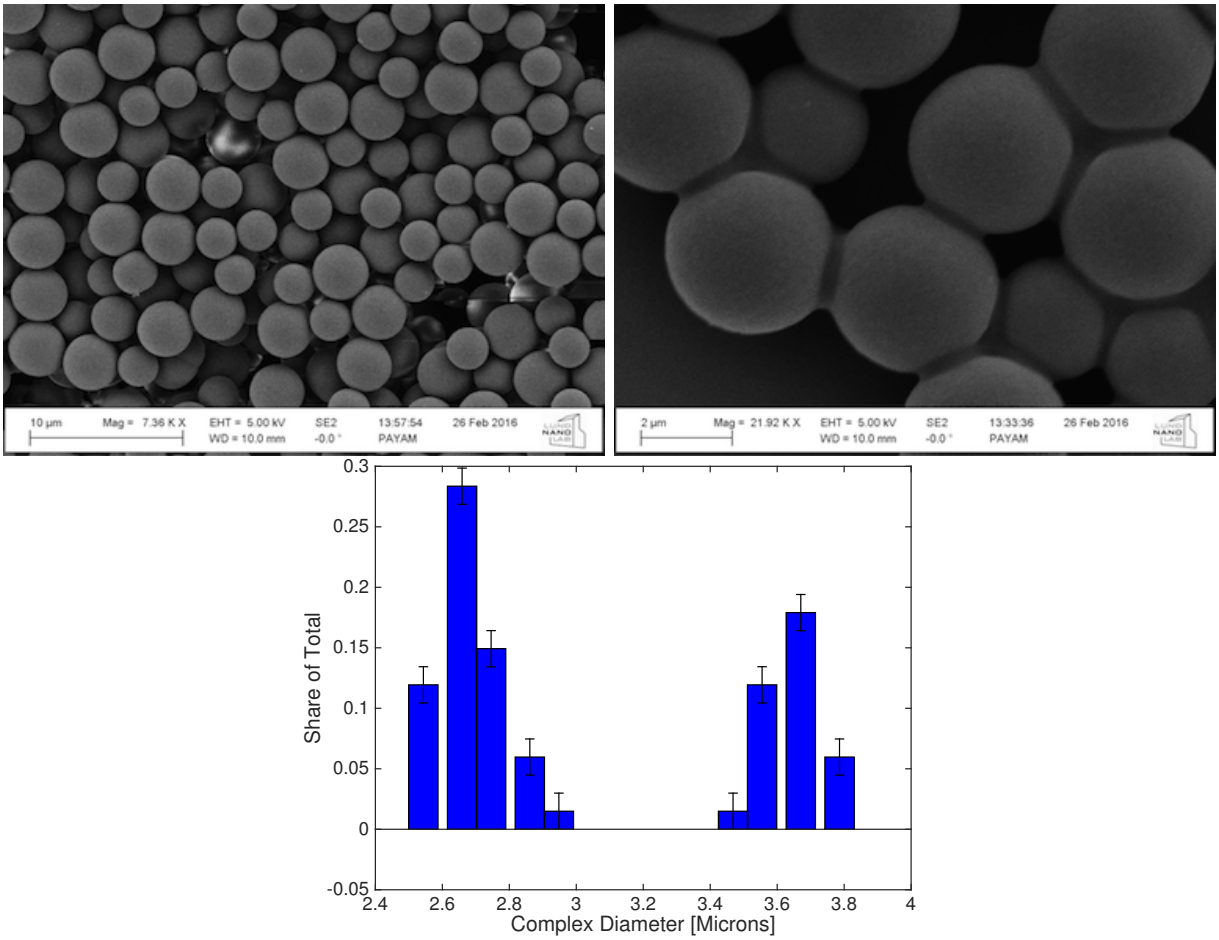

Figure 12: SEM images of the polymer-embedded catalyst complexes extracted after the third reaction cycle along with its size distribution histogram with a sample size of 67. Scale in the bottom left corner is given for size comparisson.

After the third reaction cycle minor alterations are observed. The catalyst complexes seem to be a bit more ragged and the size analysis reveals a increase in the average diameter of the complexes since no complexes smaller than 2.5 µm are observed. The closeup image to the right also show some sort of merging between the complexes not identified after the earlier reaction cycles. This effect could either be the loss of structural integrity of the complex or an effect from the resolution limitation of the scanning electron microscope. If the catalyst complexes lose their structural integrity one would expect a reduction of the complex size. However, this is not the case since the same distributions as seen for the earlier reaction cycles are observed. One could argue that the center of the distributions have been moved up by 0.1 - 0.2 µm but due to the small sample size this is within statistical error margins.

On the premise that the smaller catalyst complexes are dissoving after the third reaction cycle,

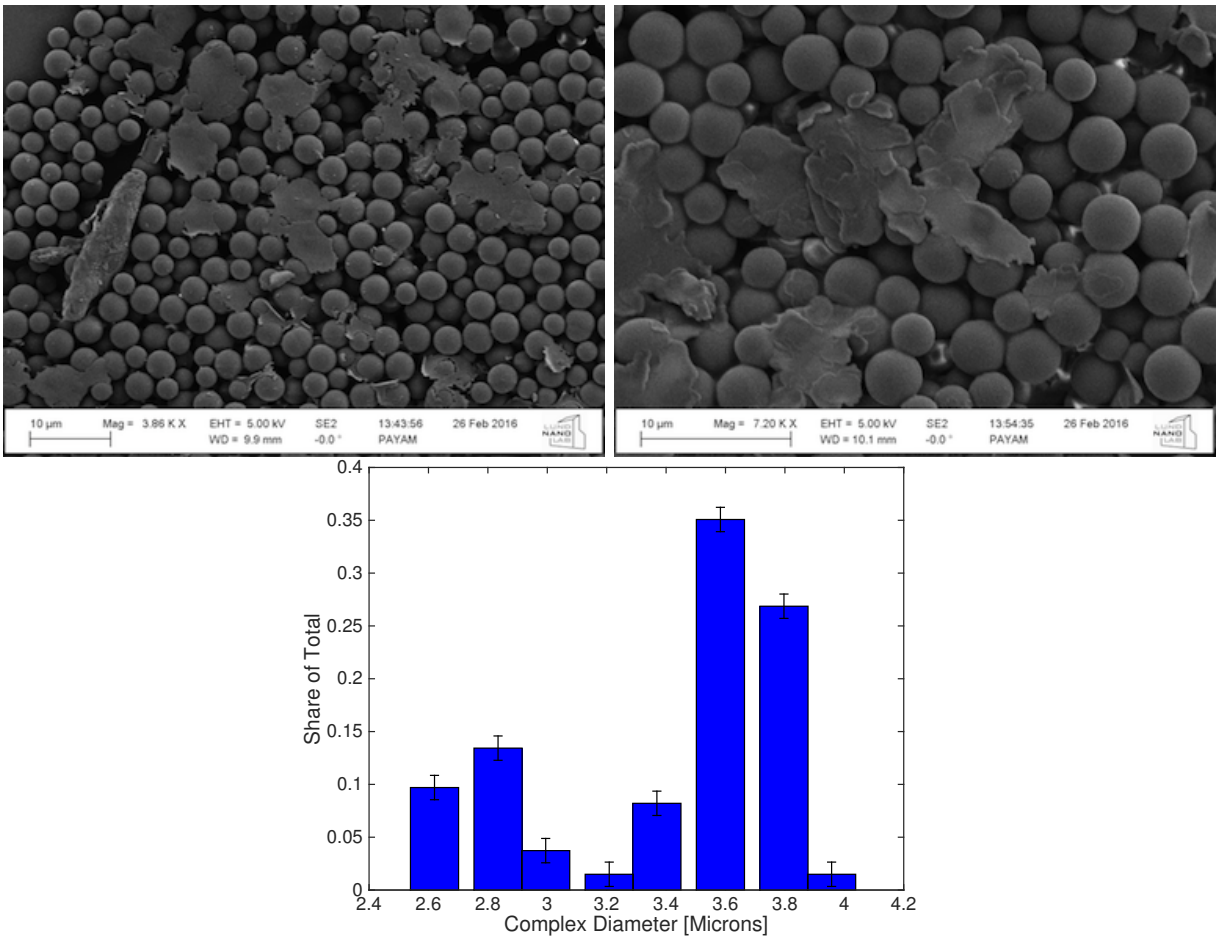

Figure 13: SEM images of the polymer-embedded catalyst complexes extracted after the fourth reaction cycle along with its size distribution with a sample size of 134. Scale in the bottom left corner is given for size comparisson.

it is only natural to assume that the spread out material seen in figure 13 are dissolved catalytic complexes. However, the material seen on top of the complexes can also be residue from the extraction procedure where other material than the catalytic complexes were extracted. Looking at the size analysis of the complexes one could suspect the material to be originating from the catalyst complexes of smaller diameter since they are not observed in the size analysis diagrams in Appendix 1. However, if this were to be the case, the same residue material would be seen after the third cycle which it is not.

4 Conclusions

Even though the full goal of examining the bonding characteristics of the linker molecule on the model silicon oxide system by the use of STM was not achieved, valuable information for further studies was made. The clean Si(001) (2×1) reconstruction shown in figure 7 and 8 gives an clear indication that the cleaning procedure was successful and a new oxide layer should be able to be constructed on the silica surface. However, due to a contamination problem with the setup a few monolayer thick oxide could not be observed postponing the linker molecule deposition. In future studies a chamber with a seperate preparation chamber is to be recommended since this was one of the main factors an ideal pressure in the chamber could not be achieved. The long-term goal of attaining a reusable molecular catalyst with improved selectivity using this method is not within the scopes for the near future. This study does, however, help in preparation for future endeavors.

The SEM measurments done on the polymer-embedded catalysts were more of a success and gave information regarding the reuseability of the catalyst. In figures 10 to 13 the catalyst complexes are shown and a size analysis of the catalysts reveal two main size-groups, in the range of 2 - 4 µm, not changing between reaction cycles. However, after the third and fourth reaction cycle some structural changes of the complexes are seen. After the third and fourth cycle no catalyst complexes are detected below 2.5 µm suggesting this could be the cause of the alterations seen after these cycles. Due to the small sample size of the size analysis this cannot be said with certainty, though he changes are instead attributed to originate from resolution limitations and isolation difficulties in the extraction procedure. These results suggest a reuseability of four times have been successfully induced for the polymer embedded catalysts. However, more studies are required to determine the origins of the meterial seen after the third and fourth cycle.

5 References

[1] P. Anastas and J. Warner. *Green Chemistry: Theory and Practice*. Oxford [England]; New York: Oxford University Press, 1998.

[2] C. Copéret, M. Chabanas, R. Petroff Saint-Arroman, and J. M. Basset. Homogeneous and Heterogeneous Catalysis: Bridging the Gap through Surface Organometallic Chemistry. *Angewandte Chemie International Edition*, 42:156–181, 2003.

[3] A. Gottlieb and L. Wesoloski. Bardeen's tunnelling theory as applied to scanning tunnelling microscopy: a technical guide to the traditional interpretation. *Nanotechnology*, 17:R57–R65, 2006.

[4] M. N Hopkinson, C. Richter, M. Schedler, and F. Glorius. An overview of N-heterocyclic carbenes. *Nature*, 510:485–496, 2014.

[5] R. Johnson, A. Hultqvist, and S. Bent. A brief review of atomic layer deposition: from fundamentals to applications. *Materials Today*, 17:236–246, 2014.

[6] B. E. Leach, editor. *Applied Industrial Catalysis*, volume 1. Academic Press, 1983.

[7] L. Lefort, M. Chabanas, O. Maury, D. Meunier, C. Coperet, J. Thivolle-Cazat, and J. M. Basset. Versatility of silica used as a ligand: effect of thermal treatments of silica on the nature

of silica-supported alkyl tantalum species. *Journal of Organometallic Chemistry*, 593:96–100, 2000.

[8] S. Muratsugu and M. Tada. Molecularly Imprinted Ru Complex Catalysts Integrated on Oxide Surfaces. *Accounts of Chemical Research*, 46:300–311, 2013.

[9] Royal Society of Chemistry. Green chemistry (url).

[10] T. W. Pi, J. F. Wen, C. P. Ouyang, R. T. Wu, and G. K. Wertheim. Oxidation of Si(001)-2 x 1. *Surface Science*, 478:L333–L338, 2001.

[11] J V Seiple and J P Pelz. Scanning Tunneling Microscopy study of Oxide Nucleation and Oxidation-Induced Roughening at Elevated Temperatures on the Si(001)-(2 x 1) Surface. *Physical Review Letters*, 73:999–1002, 1994.

[12] O Snezhkova, E Bolbat, F Ericson, P Shayesteh, S Chaudhary, N Johansson, A R Head, P Persson, O F Wendt, and J Schnadt. Structure, stability and catalytic activity in CH activation of supported NHC-Pd complexes. *Unpublished*.

[13] S. Swapp. Scanning Electron Microscopy (SEM) (url).

[14] H. Tissot, J.-J. Gallet, F. Bournel, D. Pierucci, M. Silly, F. Sirotti, and F. Rochet. Dissociation of Ethoxysilane and Methoxysilane on Si(001)-2 x 1 and Si(111)-7 x 7 at Room Temperature: A Comparative Study Using Synchrotron Radiation Photoemission. *The Journal of Physical Chemistry C*, 118:24397–24406, 2014.

[15] Wikipedia. Scanning Electron Microscopy (url), April 2016.